

Q-STAC: Q-Guided Stein Variational Model Predictive Actor-Critic

Shizhe Cai¹, Jayadeep Jacob¹, Zeya Yin¹, and Fabio Ramos^{1,2}

¹University of Sydney

²Nvidia

Abstract—Deep reinforcement learning has shown remarkable success in continuous control tasks, yet often requires extensive training data, struggles with complex, long-horizon planning, and fails to maintain safety constraints during operation. Meanwhile, Model Predictive Control (MPC) offers explainability and constraint satisfaction, but typically yields only locally optimal solutions and demands careful cost function design. This paper introduces the Q-guided Stein variational model predictive Actor-Critic (Q-STAC), a novel framework that bridges these approaches by integrating Bayesian MPC with actor-critic reinforcement learning through constrained Stein Variational Gradient Descent (SVGD). Our method optimizes control sequences directly using learned Q-values as objectives, eliminating the need for explicit cost function design while leveraging known system dynamics to enhance sample efficiency and ensure control signals remain within safe boundaries. Extensive experiments on 2D navigation and robotic manipulation tasks demonstrate that Q-STAC achieves superior sample efficiency, robustness, and optimality compared to state-of-the-art algorithms, while maintaining the high expressiveness of policy distributions. Experiment videos are available on our website: <https://sites.google.com/view/q-stac>

Index Terms—reinforcement learning, probabilistic inference, model predictive control, robotic manipulation, Stein variational inference.

I. INTRODUCTION

REINFORCEMENT Learning (RL) is often used to learn effective solvers for complex control problems, ranging from navigating cars through unknown areas to manipulating objects in various scenarios. The superiority of RL lies in its ability to handle non-linear and complex dynamics without the need for explicit modeling of robot dynamics. RL can also learn policies that are adaptive to changing environments due to the highly expressive nature of the neural networks (NN).

However, training RL policies is notably data inefficient. The number of simulation steps required for training policy networks are measured in millions for relatively simple control problems and grow rapidly for harder problems. Moreover, providing a formal, safety guarantee for the learned policy is difficult.

Model Predictive Control (MPC) is widely adopted as a robust solution within many control applications. Compared to RL, it requires accurate dynamic models that represent the controlled systems mathematically and predicts a finite horizon

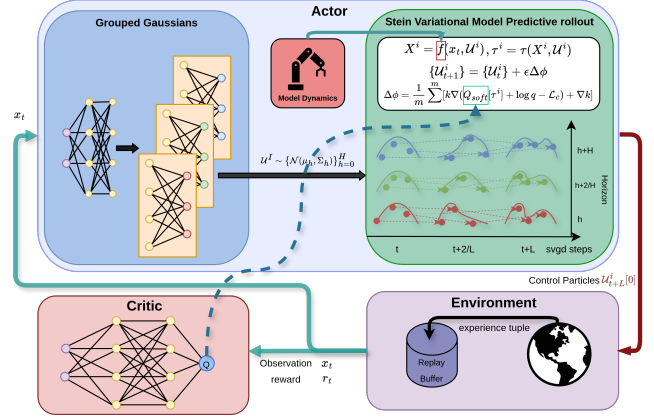


Fig. 1. A comprehensive framework of our proposed algorithm: Q-STAC. The architecture consists of four main parts: (1) an Actor initializes prior distributions from networks and sample control particle trajectories from them. (2) Control particles optimized by inference Bayesian MPC with SVGD based on Q-values, (3) a Critic network for Q-value estimation, (4) an Environment module containing the agent interaction to achieve goal state.

of system states based on the control sequence and initial states. Given a predefined cost function, MPC optimizes the control sequence by iteratively optimizing the controls within a shorter finite-horizon sequence until it reaches the goal state. The MPC schema provides explainable solutions when predicting future system behavior and can handle various constraints explicitly. Nevertheless, MPC methods only optimize finite-horizon control at each step, leading to locally optimal solutions. Moreover, to design cost functions effectively for various tasks and accurately formulate optimization problems with various constraints, both domain knowledge and control expertise are essential.

Despite their strengths, combining the high expressiveness of RL with the safety and explainability of MPC remains an open challenge in general control problems. Current hybrid approaches either learn dynamics models for RL enhancement [1]–[5], or use RL-derived functions or policies to inform MPC’s cost function and initialization [6]–[8]. However, the fundamental problem is developing an end-to-end control framework that maintains the safety and interpretability of model-based methods while preserving the expressiveness and optimality of RL approaches without requiring explicit cost function design.

In this paper, we propose a new RL algorithm, Q-guided Stein variational model predictive Actor-Critic (Q-STAC),

that addresses the aforementioned problem. As illustrated in Figure 1, at each timestep, Q-STAC initializes prior Gaussian distributions over the current observation from the network, and samples a set of particles representing the finite horizon control sequence from the initial distribution. Then, it employs a probabilistic MPC to optimize the control particles via Stein Variational Gradient Decent [9] (SVGD) based on the soft Q-value. We implement a Lagrange Multiplier to constrain SVGD updated particles to be within a specific range to avoid gradient explosion. The first control signal of each control sequence is then chosen as the grounded output of the actor and applied to the environment. We follow the standard Soft Actor-Critic (SAC) training schema for updating the actor and critic networks.

Our Q-STAC performs MPC directly on the soft Q-value learned by the critic function, eliminating the need to define the cost function explicitly. Furthermore, instead of training the RL model from scratch, leveraging the existing model dynamics as prior knowledge makes the training more data efficient. The MPC constrains ensures the control signal to be within safe boundaries. In addition, optimizing the sampled particles using constrained SVGD helps preserve the high expressiveness of the target policy distribution and maintain training stability. We experimented with several control problems to certify the effectiveness of our proposed method, including 2D particle navigation problems and robotic manipulation problems. Compared with multiple RL baseline algorithms, we show that our Q-STAC is more sample-efficient and often generates robust and safe solutions.

In summary, our Q-STAC framework brings several contributions to the field:

- A novel actor-critic architecture that directly optimizes control sequences via constrained Stein-MPC using soft Q-value as optimization rewards;
- A method to integrate system dynamics models and safety constraints within MPC, while maintaining a distribution of solutions through Stein variational inference;
- Extensive experiments on 2D navigation and robotic manipulation tasks demonstrating that Q-STAC achieves superior sample efficiency, robustness, and optimality compared to state-of-the-art baseline algorithms.

II. RELATED WORKS

RL-MPC Methods with Learnable Dynamic Models.

Modern studies have proposed to complement RL with MPC. [1]–[4] learn a bootstrap ensemble of probabilistic model dynamics and leverage the power of MPC in different ways. [1] generated short rollouts for policy updating using the learned dynamics. [2] mixtures true dynamic and model predictive rollout experience for model updating. [3] samples action using CEM methods, propagates states with trajectory sampling on the learned model, then optimizes the sampled actions and executes the best first action. [4] adds additional Gaussian Mixture Models as action ensembles and makes variational inferences in the context of model predictive rollouts. In addition, TD-MPC [5] learns a task-oriented latent dynamic model and a value function with temporal difference

learning, then performs trajectory optimization. In contrast, our method does not learn the system dynamics but utilizes it as a constraint to direct model updates; we then utilize SVGD to optimize control particles towards the target distribution via model predictive rollout.

RL-MPC Methods with Existing Dynamic Models. Several works leverage existing dynamic models to enhance the performance of RL policies with MPC [6]–[8]. [6] employs an offline RL algorithm that uses its value function as the MPC cost, then generates optimal actions using MPC online planning. [7] proposes to generate a cost map with RL policy, then coach the DiffMPC [10] with the map. [8] warm-starts the MPC with the Actor-Critic (AC) algorithm by jointly computing the predefined cost function and the value function from the AC as terminal cost. Our methods also utilize the power of dynamic models to predict future states for planning. However, we use the soft Q-value from SAC to direct Stein variational inference for Bayesian MPC, thus naturally combining the RL algorithm with MPC within a probabilistic framework.

SVGD-related Methods. Probabilistic inference helps control systems manage environmental and measurement uncertainties. SVGD [9] reformulates inference as an iterative update process and optimizes particles to approximate the target distribution. Various approaches have extended SVGD: SVPG [11] optimizes a population of policy parameters using SVGD. SVES [12] adapts SVGD to evolutionary search methods. SVMPC [13] and DuSt-MPC [14] apply it to Bayesian MPC for robust control. CSVTO [15] utilizes O-SVGD [16] for trajectory optimization over a set of trajectories while preserving system constraints. [17] proposes to combine Probabilistic Movement Primitives (ProMPs) with SVGD to handle multimodal trajectories for robot motion generation. Di-Plan [18] combines SVGD with diffusion models as informative priors and integrates path signatures to enhance diversity in the generated trajectories. Our work draws inspiration from the S²AC study [19], which integrates SVGD into SAC by sampling action particles from an initial distribution followed by SVGD updates. In contrast, we use constrained SVGD to infer a control horizon with particles initially sampled from the actor network.

III. PRELIMINARIES

A. Soft Actor-Critic

Our study builds on SAC [20], which inherits the Maximum Entropy Reinforcement Learning (MaxEnt RL) framework [21] that addresses the learning process in a continuous action space. We formulate the problem as a policy search in an infinite-horizon Markov decision process (MDP) [22] that can be expressed as a tuple $(\mathcal{S}, \mathcal{A}, p, r)$ where \mathcal{S} stands for observation space and \mathcal{A} for action space, both continuous. The state transition function $p : \mathcal{S} \times \mathcal{A} \times \mathcal{S} \rightarrow [0, \infty)$ takes the current state $s_t \in \mathcal{S}$ and action $a_t \in \mathcal{A}$ and outputs the probability density of the next state $s_{t+1} \in \mathcal{S}$. The reward term $r : \mathcal{S} \times \mathcal{A} \rightarrow [r_{min}, r_{max}]$ obtained from the environments represents a quantitative measurement of the action executed in certain states.

The goal of MaxEnt RL is to learn a policy $\pi_\varphi(a_t|s_t)$ parameterized by φ to maximize the expected cumulative reward as well as the entropy for each state,

$$J_\pi = \sum_{t=0}^T \mathbb{E}_{(s_t, a_t) \sim \rho_\pi} [r(s_t, a_t) + \alpha \mathcal{H}(\pi(\cdot|s_t))], \quad (1)$$

where α is the temperature of the entropy term, ρ_π are the marginals of trajectory distribution under policy π , and $\mathcal{H}(\pi(\cdot|s_t)) = -\sum_{a_t} \pi(a_t|s_t) \log \pi(a_t|s_t)$ is the entropy of policy at s_t state. Maximizing entropy \mathcal{H} leads to more diverse action outputs from the learned policy, thereby improving exploration efficiency and increasing sampling effectiveness.

To make the policy distribution more expressive, the policies are modeled as Energy-based Models (EBMs) $\pi(a_t|s_t) \propto \exp(-\xi(s_t, a_t))$ where $\xi(s_t, a_t)$ is an energy function and is often set to $-\frac{1}{\alpha} Q_{soft}(s_t, a_t)$. In SAC, $Q_\theta = Q_{soft}$ is parameterized by θ and represents the expected cumulative future rewards over the state-action pair. It can be learned by minimizing the mean squared error over all sampled experience from the replay buffer D ,

$$J_Q(\theta) = \mathbb{E}_{(s_t, a_t) \sim D} \left[\frac{1}{2} (Q_\theta(s_t, a_t) - \hat{Q}(s_t, a_t))^2 \right],$$

with $\hat{Q}(s_t, a_t) = r(s_t, a_t) + \gamma \mathbb{E}_{s_{t+1} \sim D} [V_{\bar{\theta}}(s_{t+1})]$

$$V_{\bar{\theta}}(s_{t+1}) = \mathbb{E}_{a_{t+1} \sim D} [Q_{\bar{\theta}}(s_{t+1}, a_{t+1}) + \alpha \mathcal{H}(\pi(\cdot|s_{t+1}))], \quad (2)$$

where $\bar{\theta}$ is the exponentially moving average of the value network weights [20] and γ is the reward discount factor. The overall objective is to minimize the expected KL-divergence between the current policy distribution and the target distribution normalized by Z :

$$J_\pi(\varphi) = \mathbb{E}_{s_t \sim D} \left[D_{KL}(\pi_\varphi(\cdot|s_t) || \frac{\exp(Q_\theta(s_t, \cdot))}{Z}) \right]. \quad (3)$$

B. Bayesian Model Predictive Control

1) *Model Predictive Control (MPC)*: MPC [23] aims to predict the system performance during a short-time horizon, thereby enabling optimal system control. The system is modeled as a state transition function $x_{t+1} = f(x_t, u_t)$ that takes as input the current system state x_t and control signal u_t , to determine the next system state. Considering a short horizon H , $X_t \triangleq (x_t, x_{t+1}, \dots, x_{t+H})$ denotes the future system states up to $t+H$. $\mathcal{U}_t \triangleq (u_t, u_{t+1}, \dots, u_{t+H-1})$ denotes a sequence of control signals indexed by t . The objective of MPC is to find a policy $\pi(x_t; f)$ that minimizes a predefined cost function $C(X_t, \mathcal{U}_t) = \{c(x_t, u_t), c_{term}(x_t)\}$ over the horizon H :

$$J(\pi) = \min \sum_{h=0}^{H-1} c(x_{t+h}, u_{t+h}) + c_{term}(x_{t+H}) \quad (4)$$

where $c(\cdot, \cdot)$ and $c_{term}(\cdot)$ are the costs for state-control pairs and termination states. At each timestep, MPC solves the optimization problem and obtains the optimal control sequences for the optimal policy $\mathcal{U}_t^* \sim \pi^*(x_t; f)$. It then executes the first control signal u_t^* in the system.

2) *MPC as Bayesian Inference*: To reason about the uncertainty in the space of solutions, MPC can be further formulated within a probabilistic framework. Specifically, following the definition in [13], [14], [24], we derive MPC as Bayesian Inference. Let $\tau = (X_t, \mathcal{U}_t)$ represent the state-control trajectory and $\mathcal{O}_\tau \in \{0, 1\}$ a binary random variable indicating the optimality of the trajectory. We can express the posterior distribution of the policy parameters φ for the policy π_φ , conditioned on the optimal trajectory (we omit $\mathcal{O}_\tau = 1$ as \mathcal{O}_τ for simplicity), system dynamics f , and the current state x_t with Bayes' rule,

$$p_t(\varphi | \mathcal{O}_\tau; f, x_t) = \frac{p_t(\mathcal{O}_\tau | \varphi; f, x_t) p_t(\varphi; x_t)}{\int p_t(\mathcal{O}_\tau | \varphi; f, x_t) p_t(\varphi; x_t) d\varphi}, \quad (5)$$

$$\propto p_t(\mathcal{O}_\tau | \varphi; f, x_t) p_t(\varphi; x_t).$$

The likelihood $p_t(\mathcal{O}_\tau | \varphi; f, x_t)$ is calculated as the marginal probability over all possible state-control pairs being optimal. Given a deterministic system dynamics, we can express the likelihood as the expectation of the optimal trajectories under policy π_φ :

$$p_t(\mathcal{O}_\tau | \varphi; f, x_t) = \int p(\mathcal{O}_\tau | \tau) p(\tau | \varphi; x_t) d\tau \quad (6)$$

$$= \mathbb{E}_{\pi_\varphi} [p(\mathcal{O}_\tau | \tau)].$$

C. Stein Variational Gradient Descent

Variational Inference (VI) allows us to approximate the target distribution p with a candidate (variational) distribution q by minimizing the Kullback-Leibler (KL) divergence $q^* = \arg \min_{q \in \mathcal{Q}} D_{KL}(q || p)$. However, typical variational inference requires the selection of an appropriate target distribution family which can be difficult for problems with multi-modal distributions. SVGD [9] offers an efficient way to approximate complex posterior distributions with a set of particles $\{\theta^i\}_{i=1}^m$. First, the particles are initialized randomly, then given a small step size ϵ , the particles are updated iteratively by

$$\theta^i \leftarrow \theta^i + \epsilon \phi^*(\theta^i), \quad (7)$$

where ϕ^* is the optimal direction of perturbation in the unit norm reproducing kernel Hilbert space (RKHS) with kernel $k(\theta', \theta)$ and acts as the gradient descent direction of the KL-divergence. We can get the close-form estimation over the mean of a group of particles:

$$\hat{\phi}^*(\theta^i) = \frac{1}{m} \sum_{j=1}^m [k(\theta^j, \theta^i) \nabla_{\theta^j} \log p(\theta^j) + \nabla_{\theta^j} k(\theta^j, \theta^i)], \quad (8)$$

where the first term represents an ‘‘attractive force’’ that directs the particles to high-probability mass regions, while the second applies a ‘‘repulsive force’’ to prevent particle collapse.

IV. METHODOLOGY

A. Q-Guided Stein Variational Model Predictive Actor-Critic

We propose a novel algorithm named Q-guided STEin variational model predictive Actor-Critic (Q-STAC) that connects SAC with Bayesian MPC via Stein Variational Inference. Our method formulates SAC policy as a Bayesian inference

problem, where we aim to find the posterior of the optimal policy given an initial prior policy distribution. Specifically, we sample a horizon of initial control particles from a group of parameterized Gaussian distributions. Then, iteratively, we perform model predictive rollout and collect state trajectories based on the dynamic model, given the initial states and control sequences. After, we compute the soft Q-value of the state-control trajectory pairs and direct the SVGD updates on control particles toward optimizing the soft Q-value.

To prevent the initial sampled particles from getting too dispersed, which could destabilize the non-smoothed landscape of the soft Q-function and potentially trigger gradient explosion, we constrain the particle to be within three standard deviations from the mean of the initial distribution, similar to [19]. However, unlike S²AC, which requires additional computation and memory, we propose constraining particle updates with an augmented Lagrangian approach. Thus, during SVGD updates, outlier particles will be pushed back to the boundaries.

From the SVGD-optimized particles, the optimized control sequence is chosen as follows: a particle is randomly selected during training for better exploration, while the particle with the maximum Q-value is selected during inference for best performance. We execute the first control signal of the sequence as the output of the RL policy. Thus, the RL policy is constrained by the knowledge of the system dynamics. We follow [19] to compute the policy's entropy in closed-form after SVGD updates. Then we follow SAC [20] to update actor and critic network. The complete algorithm is illustrated in Algorithm 1. In the following, we describe each part of the method in detail.

B. Gaussian Initialization

To enable faster convergence of the particles representing the control trajectory, we initialize the particles representing the policy distribution q_φ^0 as a set of Gaussians $\{\mathcal{N}(\mu_h, \Sigma_h)\}_{h=1}^H$, where H is the trajectory length. A sequence of means $\mu_h \triangleq (\mu_1, \mu_2, \dots, \mu_H)$ and diagonal covariances $\Sigma_h \triangleq (\sigma_1, \sigma_2, \dots, \sigma_H)$ are obtained by conditioning an MLP on the current observation x_t , $(\mu_h, \Sigma_h) = \text{MLP}_\varphi(x_t)$, where the MLP is parameterized by φ . We then sample the initial particles representing the control trajectory from the set of Gaussians:

$$\begin{aligned} \{\mathcal{U}^i\}_{i=1}^m &\triangleq \{(u_1^i, u_2^i, \dots, u_H^i)\}_{i=1}^m \\ &\sim \{\mathcal{N}(\mu_h, \sigma_h)\}_{h=1}^H \end{aligned} \quad (9)$$

where \mathcal{U}^i represents a single particle, and we abbreviate $\{\mathcal{U}^i\}_{i=1}^m = \mathcal{U}^I$ for convenience. As discussed in [19], we hope to learn an initial distribution that is close to the target distribution. The sampled particles are then progressively shifted to high density regions of the target distribution after a few SVGD update steps.

C. Stein Model Predictive Inference with Soft Q-value

We employ a nonparametric Bayesian MPC framework that optimizes directly on sampled control trajectories \mathcal{U}^I , allowing robust performance under uncertainty. Given state x , a collection of trajectories $\tau = \{\tau^i\}_{i=1}^m = \{(X^i, \mathcal{U}^i)\}_{i=1}^m$ can

be obtained by rolling out the control particles following the dynamic model $X^i = f(x, \mathcal{U}^i)$. The posterior in Eq.(5) for individual particles is proportional to the trajectory optimality likelihood multiplied by the prior distribution:

$$p(\mathcal{U}^i | \mathcal{O}_\tau; f, x) \propto p(\mathcal{O}_\tau | \tau^i) q_\varphi^0(\mathcal{U}^i; x). \quad (10)$$

In this context, deriving the optimal maximum entropy policy $\pi_\varphi^*(a|s)$ is equivalent to solving a trajectory optimization problem via approximate inference of the posterior distribution.

We employ Stein variational inference to approximate the posterior distribution [9], [13], [14], and use the soft Q-value to guide the update of SVGD. Specifically, we represent the trajectory optimality likelihood by summarizing soft Q-value over trajectories $p(\mathcal{O}_\tau | \tau^i) \propto Q_{\text{soft}}[\tau^i]$ where $Q_{\text{soft}}[\tau^i] = \sum_{h=0}^H Q_{\text{soft}}(x_{t+h}^i, u_{t+h}^i)$. Intuitively, a larger soft Q-value over a trajectory means higher probability of such trajectory being optimal and vice versa. We can further express the log-posterior by the following equation which is used to calculate $\hat{\phi}^*$ in Eq(8):

$$\begin{aligned} \log p(\mathcal{U}^i | \mathcal{O}_\tau; f, x) &= \log p(\mathcal{O}_\tau | \tau^i) + \log q_\varphi^0(\mathcal{U}^i; x) \\ &= Q_{\text{soft}}[\tau^i] + \log q_\varphi^0(\mathcal{U}^i; x). \end{aligned} \quad (11)$$

D. Constrain SVGD Update with Augmented Lagrangian

Combining RL with particle-based optimization methods such as SVGD poses a crucial challenge: particles can become extremely diverse and spread across the action space without proper constraints. Unconstrained particles compromise the numerical stability of both logarithmic probability calculations and kernel gradient computations, leading to potential training instabilities. Feeding those unscaled particles to soft Q-function may generate unexpected outputs and potentially lead to gradient explosion during training.

To mitigate training instability, we propose a constrained SVGD method that employs an augmented Lagrangian framework. Specifically, we cast SVGD as a constrained optimization problem by imposing bound constraints on the action space. For a control sequence u generated by our policy, we define the constraint function $g(u)$ as: $g(u) = \text{clamp}(u, \text{lower}, \text{upper}) - u$, where **lower** and **upper** represent the lower and upper bounds of the action space, respectively. The clamp operation restricts the value of u to lie within these bounds. In our implementation, we dynamically set these bounds relative to the prior distribution: **lower** = $\mu - 3\sigma$ and **upper** = $\mu + 3\sigma$, where μ and σ are the mean and standard deviation of the prior distribution. We can formulate the constrained optimization problem for the log-posterior as:

$$\max_{\mathcal{U}} \log p(\mathcal{U}^i | \mathcal{O}_\tau; f, x) \quad (12)$$

$$\text{s.t.} \quad g(\mathcal{U}^i) = 0, \quad i = 1, 2, \dots, m. \quad (13)$$

To solve the above we use an unconstrained objective function following the augmented Lagrangian method:

$$\mathcal{L}(\mathcal{U}^i, \lambda) = \log p(\mathcal{U}^i | \mathcal{O}_\tau; f, x) - \lambda^T g(\mathcal{U}^i) - \frac{c}{2} \|g(\mathcal{U}^i)\|^2 \quad (14)$$

where λ are Lagrange multiplier updated in the direction that increases the penalty violation: $\lambda \leftarrow \lambda + \eta \nabla_\lambda \mathcal{L}(\theta, \lambda)$, and c

is a constant penalty coefficient that determines the strength of the quadratic penalty term. We compute the gradient of the augmented Lagrangian with respect to \mathcal{U} and incorporate it into the SVGD update rule:

$$\hat{\phi}^*(\mathcal{U}^i) = \frac{1}{m} \sum_{j=1}^m [k(\mathcal{U}^j, \mathcal{U}^i) \nabla_{\mathcal{U}^j} \mathcal{L}(\mathcal{U}^i, \lambda) + \nabla_{\mathcal{U}^j} k(\mathcal{U}^j, \mathcal{U}^i)]. \quad (15)$$

Algorithm 1 Stein Model Predictive Actor-Critic

Require: Initialize parameters θ, φ , replay buffer D , dynamics f , kernel k , initial state x_0 , state transition function p
 $x_t \leftarrow x_0$

for each iteration t **do**

for each environment step **do**

$\mathcal{M}_t, \Sigma_t = \pi_\varphi(x_t)$

$\mathcal{U} \sim \mathcal{N}(\mathcal{M}_t, \Sigma_t)$

for each SVGD step **do**

 Model rollout $\tau = f(x_t, \mathcal{U})$

 Calculate $\hat{\phi}^*(\mathcal{U}^i)$ using equation (15)

 Update particle with equation (7)

end for

 Random select $\mathcal{U}^i \in \mathcal{U}$

 Pick first action $u_t \leftarrow \mathcal{U}^i[0]$

 Sample next state $x_{t+1} \sim p(x_t, u_t)$

$D \leftarrow D \cup (x_t, u_t, r_t, x_{t+1})$

end for

for each update step **do**

 Sample batched experience from D

 Calculate Entropy following [19]

 update Critic θ using Eq. (2)

 update Actor φ based on Eq. (3)

end for

end for

V. EXPERIMENTS

A. Experiment Setup

Our experiments are designed to demonstrate the sample efficiency benefits of leveraging the model dynamics. We also show that by employing MPC constrains safety and stability are improved while optimization with constrained SVGD leads to better performance than previous RL methods. We evaluate our method and compare to multiple baseline algorithms on four continuous control problems illustrated in Figure 2, for which the physical model is known. The problems are listed in the order of increasing complexity:

- The classic pendulum swing-up task;
- A 2D particle navigation problem with Gaussian obstacles, with three levels of difficulty;
- A robotic arm reaching task with cuboid obstacles;
- A robotic arm pick and place task.

The first **pendulum swing-up** problem serves as a well-understood benchmark control problem to evaluate model performance and data efficiency. As shown in Figure 2a, the task involves controlling a one-end-fixed pendulum from a random starting position to reach and remain upright by

applying torques to its free end. The system parameters include mass and gravity, which may vary during training and testing. We use the first version of the pendulum task implemented in the Gym framework [25].

Second, we implemented a **two-dimensional particle navigation** task following the OpenAI Gym API [26]. The objective is to navigate a particle to a target through a landscape of Gaussian obstacles across three difficulty levels (easy, medium, hard) that differ in obstacle quantity and positioning (Fig. 2b shows the hard level). The particle follows a double integrator dynamics, modeling a point mass under direct force control in a 2D plane. The state space comprises position (x, y) , velocity (\dot{x}, \dot{y}) , acceleration (\ddot{x}, \ddot{y}) as control inputs: $\ddot{x} = \frac{u_1}{m}, \ddot{y} = \frac{u_2}{m}$, where m is the point mass and $u = (u_1, u_2)$ represents the applied force in x and y directions. Position, speed, acceleration, and force are bounded at $\pm 10, \pm 5, \pm 10, \pm 10$, respectively. This task offers significant advantages over simple pendulum experiments: (1) it requires balancing local obstacle avoidance with global path planning, (2) it enables evaluation of both goal achievement and path quality across multiple viable solutions, and (3) its configurable parameters (particle properties, environmental friction, obstacle characteristics, and target locations) allow for customized experimental scenarios to probe learning capabilities.

The third experiment tests our algorithm in a real-world setting, where we develop **robotic manipulation** tasks in the IsaacGym [27] simulator and transfer the learned policy to a real-world Kinova Gen2 arm. The manipulator consists of an arm (with six degrees of freedom) and the three-finger gripper (with three degrees of freedom) both controlled by joint velocities in simulation. While in real, we control the gripper closure percentage. For inputs, our setup uses task-space object location coordinates directly rather than camera-based perception to focus solely on the manipulation problem and avoid the computational overhead of image processing. This design choice enables faster training iterations and helps us isolate core manipulation learning challenges from vision-related complexities.

In the reaching task, we manipulate the arm towards a target while avoiding prismatic obstacles, as displayed in Figure 2c. At each episode, we randomly initialize the start position of the arm and target position while the obstacles are fixed. There are three obstacles: two are placed close to each other so the arm can hardly navigate through them, while another is positioned to the side forming a path for the arm to pass. This task highlights the advantages of incorporating model dynamics into policy learning. When operating around physical obstacles, the model's ability to constrain the policy behavior within safe operational bounds becomes especially valuable. The presence of obstacles makes the benefits of model-guided control more evident compared to model-free approaches, as unsafe trajectories could lead to collisions with real-world consequences. Additionally, physical obstacles have clear boundaries and solid surfaces compared to Gaussian obstacles. This prevents the reinforcement learning policy from exploiting shortcuts to learn obstacle-penetrating strategies.

To further demonstrate our model's capability in highly complex control tasks, we implemented a fourth **pick-and-**

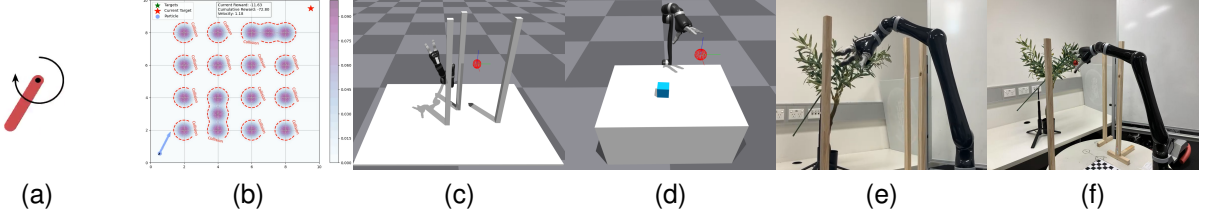


Fig. 2. Benchmark tasks used for algorithm evaluation: (a) Pendulum-V1, a classic control task involving swinging up and balancing an inverted pendulum; (b) 2D Navigation (Hard), featuring a complex navigation challenge with multiple Gaussian obstacles in a 2D space; (c) Kinova Reaching with Obstacles, where a robotic arm must reach target positions while avoiding fixed obstacles; (d) Kinova Pick and place, demonstrating a robotic manipulation task involving picking and reaching movements, and (e)(f) showing real world Kinova arm setting.

place task that aims to drive the arm to pick up a cube and then carry it to a destination, illustrated in Figure 2d. The task poses a key challenge to our method: We only have a partial model of the whole scene, specifically the kinematic model of the robot arm, whereas the dynamics of object interaction remains unknown. Through experiments, we show that despite the partial model, leveraging the robot’s dynamics as prior significantly benefits training.

B. Comparative Evaluation

We perform comparative evaluation of the tasks with multiple baseline methods. Specifically, we compare proximal policy optimization (PPO) [28], a famous on-policy policy gradient algorithm that constrains policy updates with gradient clipping, and the twin delayed deep deterministic policy gradient algorithm (TD3) [29] that employs the double Q function with delayed policy updates. However, TD3 uses a deterministic policy and relies on explicitly added noise for exploration, whereas our approach builds on an energy-based RL that strengthens exploration with entropy. Additionally, we compare against the soft actor-critic (SAC), an energy-based RL algorithm well known for its sample efficiency, and S²AC, which employs SVGD in its actor module, similar to ours. The hyperparameters for each algorithm vary between tasks. For the pendulum task, we borrow the optimized hyperparameters of PPO, TD3, and SAC from RL ZOO [30]. We use Optuna [31] to find the best hyperparameters for each algorithm in tasks where no optimized settings have been previously published. Since Q-STAC and S²AC both use SVGD to optimize control particles, they share the same set of SVGD-related parameters, while Q-STAC has the horizon length as an extra tunable hyperparameter.

Figure 3 presents the learning curves of five algorithms, PPO, TD3, SAC, S²AC, and Q-STAC on six tasks, showing their cumulative rewards over time-steps. We train each algorithm five times with different random seeds; the shaded regions denote the maximum and minimum of the cumulative rewards over these five runs, while the solid lines represent the mean rewards. The figure shows that Q-STAC outperforms PPO, TD3, and SAC over all tasks and beats S²AC when tasks get more complicated. In the pendulum task, Q-STAC and S²AC show nearly identical performance, and both converge to optimal policy faster than SAC and TD3. Due to its on-policy learning schema, PPO fails to learn an executable policy within 10000 environmental steps. In the 2D motion

planning tasks, Q-STAC consistently reaches best (medium and hard level) or near-best (easy level) final performance and shows more stable learning with fewer dramatic drops. Q-STAC achieves the highest final reward and demonstrates faster convergence in the manipulator reaching with obstacles task and Pick-and-Place tasks, significantly outperforms other methods throughout training.

C. Sample Efficiency Analysis

The primary objective of our proposed method is to enhance the sample efficiency of reinforcement learning by incorporating the model dynamics. Greater sample efficiency signifies that the model can achieve stronger learning performance with less data. To highlight the sample efficiency of our model, we conducted further analysis of the training data and generated two visual representations.

Figure 4a illustrates the percentage of environment steps required for different algorithms to reach 80% of the optimal return across six environments. As observed, in all tasks except the Pendulum task, where Q-STAC and S²AC require similar environment steps, Q-STAC consistently requires fewer environment interactions to achieve satisfactory task performance. In the reaching task, Q-STAC requires only 68.8% timesteps to reach 80% optimal return, while S²AC needs 96%, and PPO, TD3, and SAC failed. The results indicate that incorporating model-based knowledge can constrain robotic arm movements, thus reducing the probability of collisions with obstacles and achieving superior performance. Moreover, in the pick and place task, none of the other methods reached 80% of the optimal return, suggesting that our approach can find better solutions in complex control problems.

Figure 4b presents a box plot of the normalized mean return values over the first 50 training episodes for each algorithm for all tasks. The results demonstrate that Q-STAC exhibits the highest mean and maximum values compared to other algorithms, suggesting that Q-STAC maintains a leading position early in the training process. Overall, Q-STAC outperforms other algorithms in terms of sample efficiency. While S²AC and SAC demonstrate competitive performance in relatively simple tasks, they generally fall short compared to Q-STAC. The on-policy PPO algorithm exhibits the lowest sample efficiency among all evaluated methods.

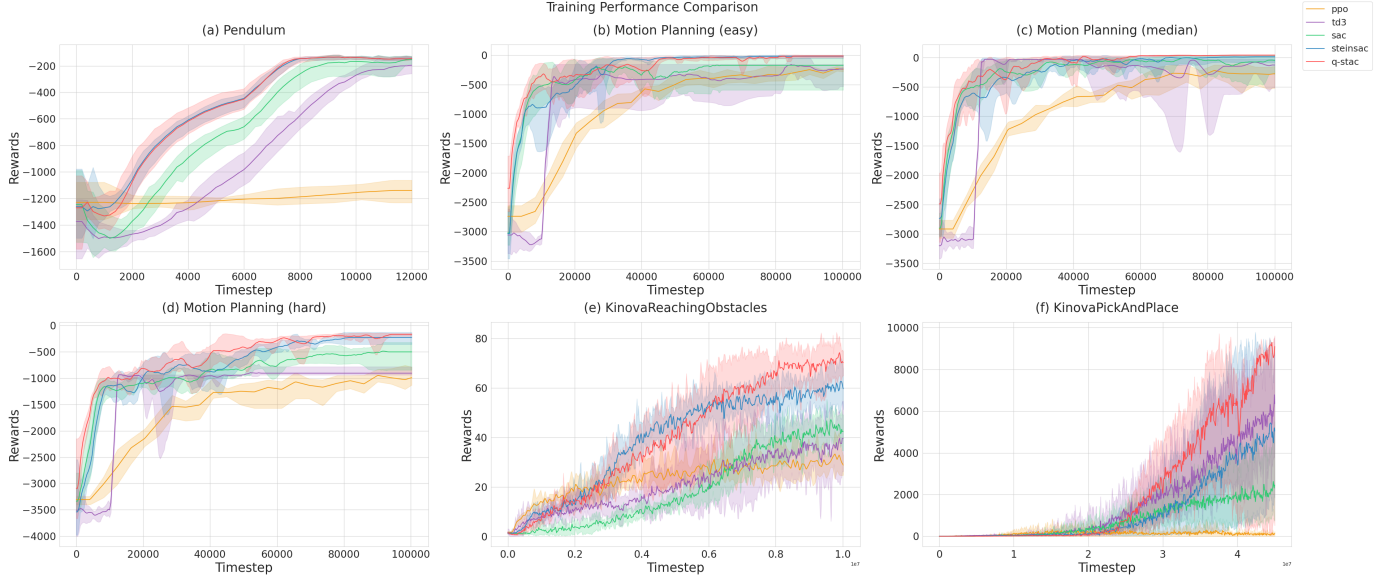


Fig. 3. Performance comparison of reinforcement learning algorithms across multiple control tasks. The figure displays training curves for five distinct algorithms (PPO, TD3, SAC, S²AC, and Q-STAC) evaluated on six benchmark environments. (a) Pendulum control task. Motion Planning with increasing difficulty levels ((b) easy, (c) medium, (d) hard), (e) KinovaReachingObstacles task and (f) KinovaPickAndPlace task. Each plot shows the cumulative reward values (y-axis) against training timesteps (x-axis), with solid lines representing mean performance and shaded regions indicating standard deviation across multiple runs.

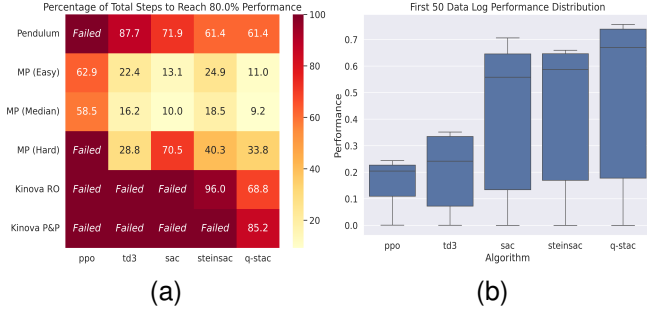


Fig. 4. (a) Sample efficiency comparison showing percentage of steps needed to reach 80% performance threshold. Lower values (lighter colors) indicate better efficiency. (b) Performance distribution of reinforcement learning algorithms across the first 50 data logs.

D. Sim-to-Real

1) *General Setup*: We perform training and inferencing on a desktop computer with an NVIDIA RTX4090 GPU. We set up the Kinova ROS API on a separate workstation and interact with it via a custom REST service through the ethernet. The control input of the Kinova arm is joint velocity, and the control rate is restrained to be around 55Hz-60Hz.

2) *Adaptive Action Integration for Robot Control*: To address the reality gap between simulation and real-world execution, we adopt a modified action integration approach inspired by [32], [33]. The gap between reality and simulation, such as friction, damping, and stiffness, often leads to steady-state error accumulated over time when transferring policies. The standard approach applies policy action $a_t = \pi(o_t)$ directly to the current state s_t : $s_{t+1}^d = s_t \oplus a_t = s_t \oplus \pi(o_t)$, where o_t is the observation, s_{t+1}^d is the next desired state and \oplus

represents state update operations. However, this approach is not robust against disturbances. [33] propose a Policy-Level Action Integrator (PLAI) to address the issue by integrating action over time: $s_{t+1}^d = s_t^d \oplus a_t = s_t^d \oplus \pi(o_t)$. The key idea is to achieve robust joint velocity control, where the accumulated joint position error often rises as the control step increases.

We thereby implemented an adaptive action integrator following [32]. Our RL policy outputs the current desired joint velocity of the 6-Dofs Kinova arm as action $a_t = \pi(o_t)$. We calculate the desired segment changes of action based on the last state and current action: $\delta a_t^d = \frac{s_t - a_t}{n}$, where n is the segment factor for feeding Kinova ROS controller in higher frequency. Then, we update the state via action integration.

$$s_{t+1}^d = s_t^d \oplus \delta a_t^d \quad (16)$$

$$s_t^d = \begin{cases} s_t & \text{if } i \% n = 0 \\ s_i^d & \text{otherwise} \end{cases}, \text{ for } i = 0, 1, 2, \dots, n$$

3) *Real Experiments*: We design a task in a real-world environment where the robotic arm moves over wooden obstacles and reaches a designated target location to pick up a fruit hanging on a tree. Such setup allows us to directly use the policy learned from the Kinova-Reaching-with-Obstacles task and perform sim-to-real policy transfer. During the phase in which the robotic arm traverses the obstacle to reach the target location, control is entirely handled online by the learned RL policy. Once the arm reaches the target, we manually close the gripper to perform the picking action. Figure 2e 2f shows our real-world task setup. Table I illustrates the success rate of all algorithms in the simulation and real-world tasks. In simulation, we conducted experiments across 1000 parallel environments and repeated 10 times using the best

TABLE I

Environments	Algorithms	Tests	
		Success Rate (%)	
Simulator Reaching with Obstacles	SAC	26.7 \pm 1.35	
	TD3	17.5 \pm 1.50	
	PPO	11.3 \pm 0.90	
	S ² AC	78.9 \pm 3.85	
	Q-STAC	83.6 \pm 3.72	
Simulator Pick and Reach	SAC	Reaching Cube	Reaching Targets
	TD3	83.5 \pm 1.43	80.9 \pm 1.51
	PPO	93.4 \pm 1.28	92.3 \pm 1.27
	S ² AC	22.2 \pm 1.72	/
	Q-STAC	93.1 \pm 1.92	82.7 \pm 1.90
Real World Picking Fruit	SAC	Avoiding Obstacles	Reaching Target
	TD3	20.0	40.0
	PPO	/	13.3
	S ² AC	13.3	33.3
	Q-STAC	86.7	60.0
		93.3	80.0

checkpoint of each algorithm to calculate the success rates. We executed each task 15 times to calculate the successful rates for real-world experiments. From the results, S²AC typically ranks as the second-best performing algorithm with strong performance, particularly in obstacle-related tasks. Q-STAC consistently demonstrates superior performance in all test environments, achieving the highest success rates in nearly every task.

VI. CONCLUSION AND FUTURE WORK

We propose Q-STAC, a novel end-to-end RL algorithm that combines Bayesian MPC and SVGD for policy learning with SAC. Our approach leverages a dynamics model as prior knowledge to guide the RL process, significantly improving its sample efficiency. By employing Stein variational inference, we obtain policies capable of representing more complex distributions, thereby enhancing their effectiveness in solving challenging tasks. Additionally, incorporating the model as a constraint contributes to the robustness and safety of the learned policies. We conduct experiments on multiple control problems ranging from particle navigation tasks to robot manipulation tasks. Compared to state-of-the-art RL algorithms, we demonstrated the superior performance of our method in complex tasks and its enhanced safety features. We perform additional sim-to-real experiments to show that our methods are robust in real-world robotic problems. For future work, we aim to integrate known robot models with learned interaction dynamics to create more accurate world models for Q-STAC, targeting more complex tasks such as cloth manipulation.

REFERENCES

- [1] M. Janner, J. Fu, M. Zhang, and S. Levine, “When to trust your model: Model-based policy optimization,” *Advances in neural information processing systems*, vol. 32, 2019.
- [2] A. S. Morgan, D. Nandha, G. Chalvatzaki, C. D’Eramo, A. M. Dollar, and J. Peters, “Model predictive actor-critic: Accelerating robot skill acquisition with deep reinforcement learning,” in *2021 IEEE International Conference on Robotics and Automation (ICRA)*. IEEE, 2021, pp. 6672–6678.
- [3] K. Chua, R. Calandra, R. McAllister, and S. Levine, “Deep reinforcement learning in a handful of trials using probabilistic dynamics models,” *Advances in neural information processing systems*, vol. 31, 2018.
- [4] M. Okada and T. Taniguchi, “Variational inference mpc for bayesian model-based reinforcement learning,” in *Conference on robot learning*. PMLR, 2020, pp. 258–272.

- [5] N. Hansen, X. Wang, and H. Su, “Temporal difference learning for model predictive control,” 2022. [Online]. Available: <https://arxiv.org/abs/2203.04955>
- [6] K. Lowrey, A. Rajeswaran, S. Kakade, E. Todorov, and I. Mordatch, “Plan online, learn offline: Efficient learning and exploration via model-based control,” *arXiv preprint arXiv:1811.01848*, 2018.
- [7] A. Romero, Y. Song, and D. Scaramuzza, “Actor-critic model predictive control,” in *2024 IEEE International Conference on Robotics and Automation (ICRA)*. IEEE, 2024, pp. 14 777–14 784.
- [8] R. Reiter, A. Ghezzi, K. Baumgärtner, J. Hoffmann, R. D. McAllister, and M. Diehl, “Ac4mpc: Actor-critic reinforcement learning for nonlinear model predictive control,” *arXiv preprint arXiv:2406.03995*, 2024.
- [9] Q. Liu and D. Wang, “Stein variational gradient descent: A general purpose bayesian inference algorithm,” *Advances in neural information processing systems*, vol. 29, 2016.
- [10] B. Amos, I. Jimenez, J. Sacks, B. Boots, and J. Z. Kolter, “Differentiable mpc for end-to-end planning and control,” *Advances in neural information processing systems*, vol. 31, 2018.
- [11] Y. Liu, P. Ramachandran, Q. Liu, and J. Peng, “Stein variational policy gradient,” 2017. [Online]. Available: <https://arxiv.org/abs/1704.02399>
- [12] C. V. Braun, R. T. Lange, and M. Toussaint, “Stein variational evolution strategies,” 2024. [Online]. Available: <https://arxiv.org/abs/2410.10390>
- [13] A. Lambert, A. Fishman, D. Fox, B. Boots, and F. Ramos, “Stein variational model predictive control,” *arXiv preprint arXiv:2011.07641*, 2020.
- [14] L. Barcelos, A. Lambert, R. Oliveira, P. Borges, B. Boots, and F. Ramos, “Dual online stein variational inference for control and dynamics,” *arXiv preprint arXiv:2103.12890*, 2021.
- [15] T. Power and D. Berenson, “Constrained stein variational trajectory optimization,” 2024. [Online]. Available: <https://arxiv.org/abs/2308.12110>
- [16] R. Zhang, Q. Liu, and X. T. Tong, “Sampling in constrained domains with orthogonal-space variational gradient descent,” 2022. [Online]. Available: <https://arxiv.org/abs/2210.06447>
- [17] Z. Yin, T. Lai, S. Khan, J. Jacob, Y. Li, and F. Ramos, “Stein movement primitives for adaptive multi-modal trajectory generation,” in *2024 IEEE/RSJ International Conference on Intelligent Robots and Systems (IROS)*, 2024, pp. 11 901–11 908.
- [18] Z. Yin, T. Lai, L. Barcelos, J. Jacob, Y. Li, and F. Ramos, “Diverse motion planning with stein diffusion trajectory inference,” *IEEE International Conference on Robotics and Automation (ICRA)*, 2025.
- [19] S. Messaoud, B. Mokeddem, Z. Xue, L. Pang, B. An, H. Chen, and S. Chawla, “S²ac: Energy-based reinforcement learning with stein soft actor critic,” 2024. [Online]. Available: <https://arxiv.org/abs/2405.00987>
- [20] T. Haarnoja, A. Zhou, P. Abbeel, and S. Levine, “Soft actor-critic: Off-policy maximum entropy deep reinforcement learning with a stochastic actor,” in *International conference on machine learning*. PMLR, 2018, pp. 1861–1870.
- [21] T. Haarnoja, H. Tang, P. Abbeel, and S. Levine, “Reinforcement learning with deep energy-based policies,” in *International conference on machine learning*. PMLR, 2017, pp. 1352–1361.
- [22] M. L. Puterman, “Markov decision processes,” *Handbooks in operations research and management science*, vol. 2, pp. 331–434, 1990.
- [23] C. E. Garcia, D. M. Prent, and M. Morari, “Model predictive control: Theory and practice—a survey,” *Automatica*, vol. 25, no. 3, pp. 335–348, 1989.
- [24] S. Levine, “Reinforcement learning and control as probabilistic inference: Tutorial and review,” *arXiv preprint arXiv:1805.00909*, 2018.
- [25] M. Towers, A. Kwiatkowski, J. Terry, J. U. Balis, G. D. Cola, T. Deleu, M. Goulão, A. Kallinteris, M. Krimmel, A. KG, R. Perez-Vicente, A. Pierré, S. Schulhoff, J. J. Tai, H. Tan, and O. G. Younis, “Gymnasium: A standard interface for reinforcement learning environments,” 2024. [Online]. Available: <https://arxiv.org/abs/2407.17032>
- [26] G. Brockman, V. Cheung, L. Pettersson, J. Schneider, J. Schulman, J. Tang, and W. Zaremba, “Openai gym,” 2016. [Online]. Available: <https://arxiv.org/abs/1606.01540>
- [27] V. Makovychuk, L. Wawrzyniak, Y. Guo, M. Lu, K. Storey, M. Macklin, D. Hoeller, N. Rudin, A. Allshire, A. Handa, and G. State, “Isaac gym: High performance gpu-based physics simulation for robot learning,” 2021. [Online]. Available: <https://arxiv.org/abs/2108.10470>
- [28] J. Schulman, F. Wolski, P. Dhariwal, A. Radford, and O. Klimov, “Proximal policy optimization algorithms,” 2017. [Online]. Available: <https://arxiv.org/abs/1707.06347>
- [29] S. Fujimoto, H. van Hoof, and D. Meger, “Addressing function approximation error in actor-critic methods,” 2018. [Online]. Available: <https://arxiv.org/abs/1802.09477>

- [30] A. Raffin, “Rl baselines3 zoo,” <https://github.com/DLR-RM/rl-baselines3-zoo>, 2020.
- [31] T. Akiba, S. Sano, T. Yanase, T. Ohta, and M. Koyama, “Optuna: A next-generation hyperparameter optimization framework,” 2019. [Online]. Available: <https://arxiv.org/abs/1907.10902>
- [32] J. Jacob, S. Cai, P. V. K. Borges, T. Bandyopadhyay, and F. Ramos, “Gentle manipulation of tree branches: A contact-aware policy learning approach,” in *8th Annual Conference on Robot Learning*, 2024. [Online]. Available: <https://openreview.net/forum?id=zc2GPi3DSb>
- [33] B. Tang, M. A. Lin, I. Akinola, A. Handa, G. S. Sukhatme, F. Ramos, D. Fox, and Y. Narang, “Industreal: Transferring contact-rich assembly tasks from simulation to reality,” 2023. [Online]. Available: <https://arxiv.org/abs/2305.17110>